



TITLE:

HYDRAULIC MODEL EXPERIMENT ON THE DIFFUSION DUE TO THE TIDAL CURRENT

AUTHOR(S):

HIGUCHI, Haruo; SUGIMOTO, Takashige

CITATION:

HIGUCHI, Haruo ...[et al]. HYDRAULIC MODEL EXPERIMENT ON THE DIFFUSION DUE TO THE TIDAL CURRENT. Special Contributions of the Geophysical Institute, Kyoto University 1966, 6: 113-125

ISSUE DATE:

1966-12

URL:

<http://hdl.handle.net/2433/178512>

RIGHT:

HYDRAULIC MODEL EXPERIMENT ON THE DIFFUSION DUE TO THE TIDAL CURRENT

By

Haruo HIGUCHI and Takashige SUGIMOTO

(Received November 16, 1966)

Abstract

The diffusion phenomena due to the tidal current in a shallow broad estuary are here studied in a hydraulic model experiment for which Ariake Bay in the Omuta area of Kyushu, was used as the prototype. Only the tidal current is taken into account, the effect of the other factors, the ocean current, density stratification, the wind, waves and so on, which may influence the diffusion in the estuary, is not considered.

A model of the northern half of Ariake Bay, with a horizontal and vertical scale of 1/2000 and 1/200 respectively, was constructed, and a semidiurnal tide generated by an automatically controlled pneumatic tide generator was provided for it. The water level at 5 stations, the current ellipses at 4 stations and the flow pattern were measured and compared with those in the prototype. The diffusion from an instantaneous point source was investigated mainly by the photographic method.

Experiments have shown that the tide and the tidal current are accurately reproduced in the model. However, the diffusion coefficient evaluated through the rate of increase of the dye patch is about 1/3 of that in the prototype. This may be due to the difference between the flow in the model and that in the prototype, the former belonging to the perfect turbulent regime and the latter to the transient regime.

1. Introduction

After the completion of new seaside industrial zones, which are now under construction or in the planning stage, it is expected that various kinds of industrial waste will be discharged into the sea so that water pollution may become a major problem. In order to execute this programme rationally it is essential to forecast its probable after effects and the hydraulic model experiment is one of the most useful means of doing so. Although there are many factors which control the diffusion phenomena in the sea, for example the ocean current, the tidal current, density stratification, waves, the wind and so on, it is only the tidal current that is taken into consideration in this study.

As to the tidal phenomena in Ariake Bay some experiments have already

been made in the Nagasaki Marine Observatory and at Kyushu University, in which the diffusion phenomenon was not treated but the change of tidal range caused by the construction of the embankment across the bay was investigated. Therefore this is the first attempt to investigate the diffusion phenomena in Ariake Bay by means of the hydraulic model experiment. In this paper the applicability of the hydraulic model experiment to the diffusion phenomena in the coastal sea area is studied through a comparison of the experimental results with field observations.

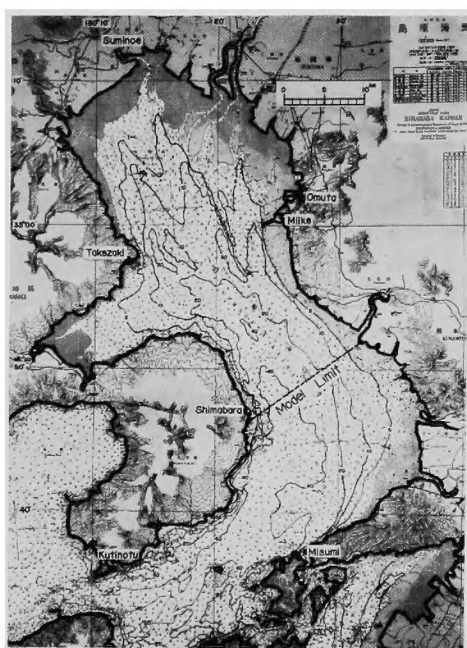


Fig. 1. Bathymographic chart of Ariake Bay.

2. Prototype

Ariake Bay is about 90 km in length, 18 km in mean width, and 20 m in mean water depth, and is connected with the open sea through the Hayasaki Straits as shown in Fig. 1. In the inner part of the bay the bottom slope is very small and the bottom material is mainly mud.

The tide in the bay is governed by that of the open sea as it passes through the straits. The tidal constituents in this area are shown in Table 1. From this table it is clear that the semidiurnal tide is predominant and that both constituents M_2 and S_2 become larger in the inner part of the bay. As for the time phase the larger lag appears within the straits and on

Table 1. Tidal constant

Constituent	M_2		S_2		K_1		O_1		Period (month)
Station	$H(\text{cm})$	$\kappa(^{\circ})$	$H(\text{cm})$	$\kappa(^{\circ})$	$H(\text{cm})$	$\kappa(^{\circ})$	$H(\text{cm})$	$\kappa(^{\circ})$	
Tomioka	96	230	43	252	27	208	20	190	1
Kuchinotsu	104	253	41	290	28	216	21	192	4
Misumi	125	254	52	295	26	220	19	201	4
Shimabara	147	258	56	299	25	219	20	204	4
Takezakijima	158	259	69	299	29	220	22	203	1
Miike	159	259	69	299	27	219	21	198	4
Suminoe	172	267	75	306	27	221	22	205	1

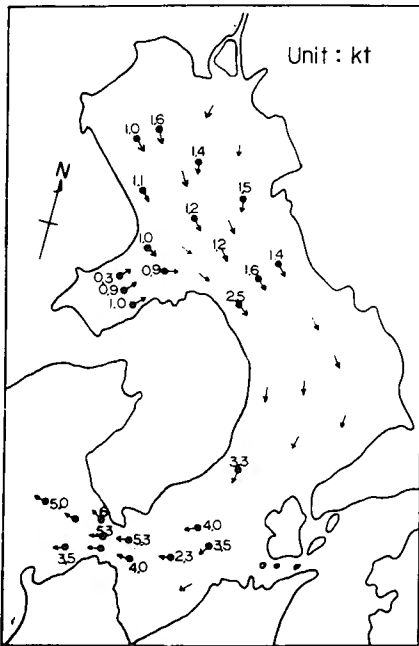


Fig. 2. Maximum tidal current in the ebb (Prototype).

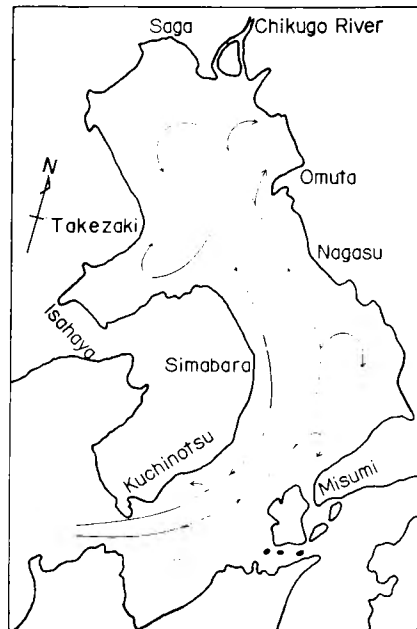


Fig. 3. General flow.

the way from the straits to the bay bottom the lag seems to be proportional to the distance but is rather small. The monthly mean sea level is highest in August and lowest in February and the difference is about 38 cm. The mean sea level in the inner part is about 30 cm higher than in the open sea.

The maximum tidal current at the ebb is shown in Fig. 2. In the flood the direction is almost the reverse and the velocity is almost the same. The general flow in the bay is mainly counterclockwise and a small clockwise circulation can be seen in the Omuta Area, on the northern side of Omuta, as shown in Fig. 3.

The flow pattern in the Omuta area is shown in Fig. 4. The velocity of the tidal current becomes great up to 2 knots or more near the head of the breakwater of Miike Harbor. The current ellipses were obtained at 4 points in this area, two of which are shown in Fig. 10. The tidal excursion is about 11 km according to the observation made after a float had been traced.

For a diffusion of smaller scale the coefficient was obtained from an observation of the dye patch in the Omuta area. The time change of the area of the dye patch 3 km off the coast and at the mouth of Omuta River is shown in Fig. 5, which was measured by means of aerial photography. In this figure the name of the mark shows the tidal phase by quadrants when the sea level may be

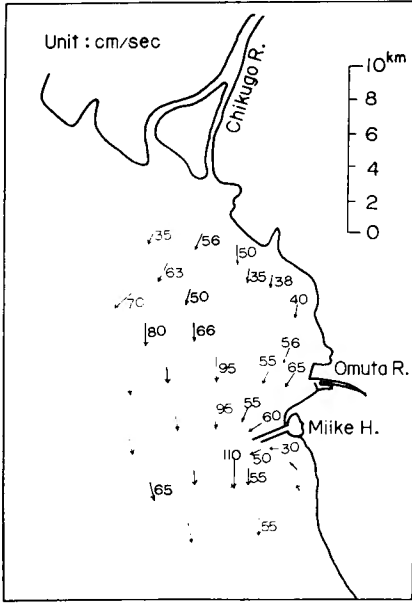


Fig. 4. Flow pattern in the Omuta Area in the ebb (Prototype).

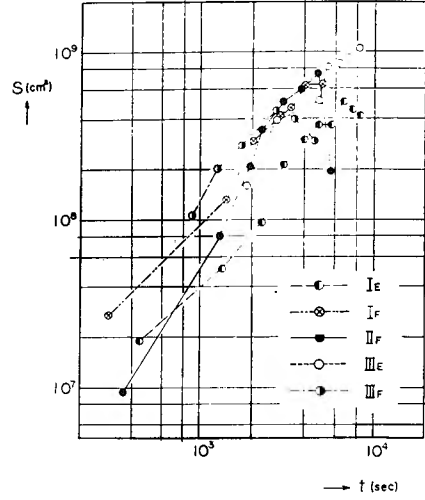


Fig. 5. Time change of the area of the dye patch in the Omuta Area.

expressed by the equation, $\zeta = \zeta_0 \sin \theta$. Therefore I shows the flood, and II and III show the ebb. The area of the dye patch increased for some hours after it was thrown, then it decreased gradually. The inverse slope on the right hand side of this figure shows the decreasing stage.

The concentration of the dye at time t in the dye patch, which had the symmetrical distribution $C = C_0 \exp\left(-\frac{r^2}{a^2}\right)$ initially, was obtained as follows,

$$C = \frac{C_0}{1 + \frac{4Kt}{a^2}} \exp\left\{-\frac{r^2}{a^2\left(1 + \frac{4Kt}{a^2}\right)}\right\}$$

from

$$\frac{\partial C}{\partial t} = K\left(\frac{\partial^2 C}{\partial x^2} + \frac{\partial^2 C}{\partial y^2}\right).$$

Supposing the same concentration at the rim of the patch the concentrations at t_{i-1} and t_i are written as follows,

$$\frac{C_0}{1 + \frac{4Kt_i}{a^2}} \exp\left\{-\frac{r_i^2}{a^2\left(1 + \frac{4Kt_i}{a^2}\right)}\right\} = \frac{C_0}{1 + \frac{4Kt_{i-1}}{a^2}} \exp\left\{-\frac{r_{i-1}^2}{a^2\left(1 + \frac{4Kt_{i-1}}{a^2}\right)}\right\}.$$

Assuming

$$\frac{1}{1 + \frac{4Kt_i}{a^2}} \sim \frac{1}{1 + \frac{4Kt_{i-1}}{a^2}}$$

and

$$\exp\left\{-\frac{r^2}{a^2\left(1+\frac{4Kt}{a^2}\right)}\right\} \sim 1 - \frac{r^2}{a^2\left(1+\frac{4Kt}{a^2}\right)},$$

the diffusion coefficient is written as follows,

$$K \sim \frac{r_i^2 - r_{i-1}^2}{4(t_i - t_{i-1})}$$

or

$$K \sim \frac{4S_i}{4\pi\Delta t_i}$$

where

$$S_i - S_{i-1} = \Delta S_i$$

and

$$t_i - t_{i-1} = \Delta t_i.$$

The relation between the diffusion coefficient K evaluated by this equation and the equivalent radius of the patch is shown in Fig. 6. The slope of the line is 4/3.

3. Similitude

In the hydraulic model experiment for the tidal current it is necessary for the following equations to be valid in order to hold a dynamic similitude between the prototype and the model,

$$t_r = x_r h_r^{-1/2}, \quad (3.1)$$

and

$$C_{fr} = x_r^{-1} h_r, \quad (3.2)$$

where x is the horizontal length, h the vertical length, t the time, C_f the drag coefficient, and where the suffix r shows the ratio of the quantity in the prototype to that in the model. When the flow in the model is in the turbulent regime and Manning's roughness coefficient is used as the frictional coefficient, the equation (3.2) is written as follows,

$$n_r = x_r^{-1/2} h_r^{2/3}. \quad (3.2)$$

Now the horizontal scale $1/x$ is determined as $1/2000$ when both the area of the prototype to be involved in the model, shown in Fig. 1 by the broken line designating the model limit, and the space of the laboratory to be used have been taken into account. Using Manning's coefficient of the prototype n_p ,

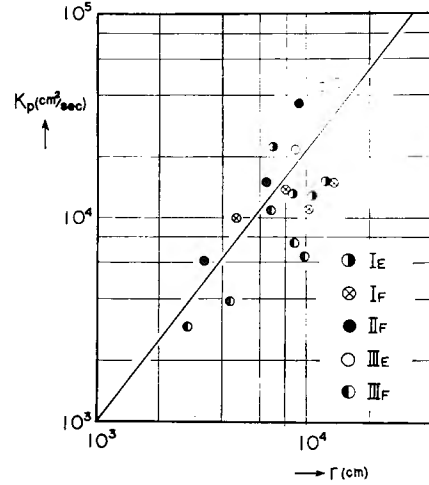


Fig. 6. Relation between the diffusion coefficient K_p and the equivalent radius r .

$=0.01$, which is reported by Nagasaki Marine Observatory, and that of the model $n_m=0.013$, we get the vertical scale $1/h_r=1/200$ by the equation (3.3). To produce the equation $n_m=0.013$, it is sufficient to make the bottom roughness of the model $k_s=1.3$ mm by using a brush on it.

The Reynolds number in the Omuta Area in the model changes according to the tidal phase. The maximum value is expected to be 3600 and the period in which the number is more than 2000 exceeds 62% of the whole period if we assume that the velocity changes sinusoidally. Therefore it can be regarded as an experiment in the turbulent regime.

It is considered that the similitude holds for the turbulence of the scale of the tidal excursion or of the tidal period among many scales of the turbulence, which contribute to the diffusion, because the similitude holds for the tidal current. However it is difficult if not impossible to simulate in the model the microstructure of the flow in the prototype. Therefore it can not be assumed that the diffusion phenomena contributed by the turbulence of every scale or period can be accurately reproduced in the model. So we can accept the results of the experiment when we can estimate the diffusion in the prototype by making certain corrections based on the relationship between the model and the prototype. Since the diffusion coefficient has the dimension of L^2T^{-1} , when the similitude holds we get $K_r=2.8 \times 10^4$ from the following equation,

$$K_r = x_r h_r^{1/2}. \quad (3.4)$$

In this paper the diffusion coefficient calculated by the equation is always discussed.

The hydraulic factors in the model are shown in Table 2.

Table 2. Hydraulic factors in the prototype and the model

	Scale	Prototype	Model
Distance	1/2000	20 km	10 m
Water depth	1/200	10 m	5 cm
Tidal range	1/200	5 m	2.5 cm
Tidal period	1/141	12h 25m	5m 17sec
Current velocity	1/14.1	1 kt	3.53 cm/sec
Discharge	$1/5.66 \times 10^6$	$10^5 \text{ m}^3/\text{day}$	$0.206 \text{ cm}^3/\text{sec}$
Diffusion coefficient	$1/2.8 \times 10^4$	$2.8 \times 10^4 \text{ cm}^2/\text{sec}$	$1 \text{ cm}^2/\text{sec}$

4. Experimental facilities

The experiment was carried out at Ujigawa Hydraulic Laboratory, Disaster Prevention Research Institute, Kyoto University.

(a) Model basin

A model of Ariake Bay as shown in Fig. 7 and Photo 1 with a horizontal scale of 1/2000 and a vertical scale of 1/200 was constructed. The limiting line of the area involved is shown by a broken line in Fig. 1. The bottom topography was reproduced to a highly accurate degree with the use of mortar. A number of crosses were drawn on the bottom at every meter to be used as a scale in measuring the current velocity.

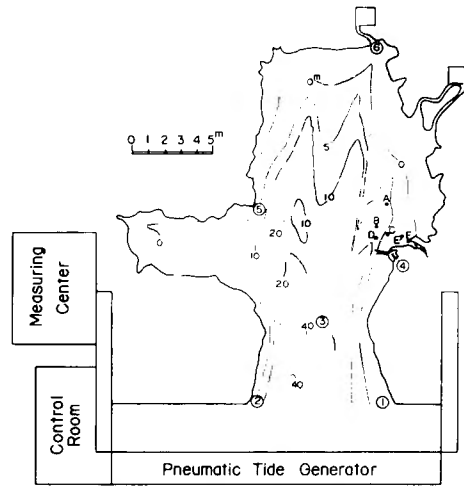


Fig. 7. Model of Ariake Bay.

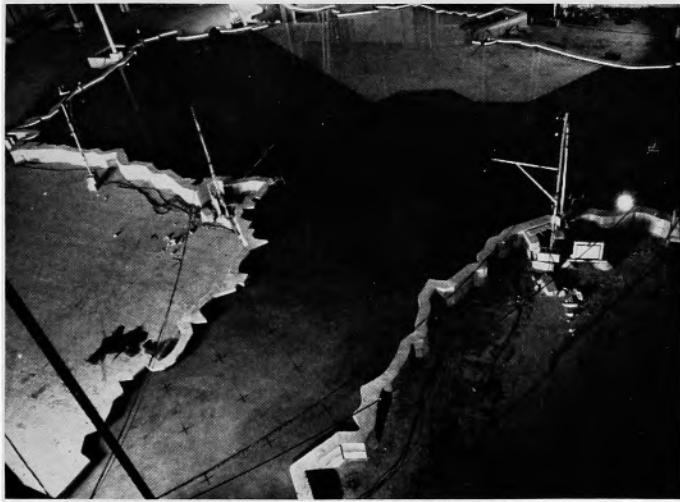


Photo. 1. Model of Ariake Bay.

(b) Tide generator

A pneumatic tide generator, which was operated by an automatic control system, was used for reproducing the semidiurnal tide. The tidal range is from 1.5 to 3 cm and the period was 5 min 17 sec.

(c) Measurement

The water level is measured at 5 points of ①, ②, etc. in Fig. 7 by

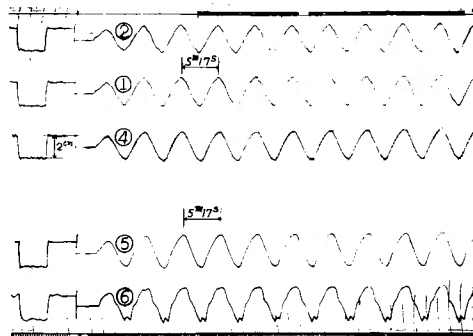


Fig. 8. Record of water level in the model.

wave meters of the electric resistance type. An example of the records is shown in Fig. 8.

The flow pattern was obtained by intermittently photographing many white floats scattered on the water surface with 35 mm cameras and a 16 mm cine camera. The time change of the visual area of the dye patch was measured in the same way.

5. Procedure

At first the experiment for examining the similitude for the tide and the tidal current was carried out by measuring the water levels, the flow pattern, and the current ellipses.

After the confirmation of the similitude, the diffusion from an instantaneous point source with the use of methylene blue was investigated.

6. Results

(a) Tide

The records of the tide were obtained as shown in Fig. 8. The result of the harmonic analysis of the records are shown in Table 3. In this table the

Table 3. Harmonic constants of the tide in the model (Run 29)

Station	①	②	④	⑤	⑥
H_1 (cm)	1.13	1.13	1.24	1.26	1.34
H_1^m, H_1^1	1.00	1.00	1.10	1.12	1.19
H_2	0.03	0.03	0.05	0.06	0.08
$\Delta\delta$	0°00'	+30'	-20'	+10'	+2°30'

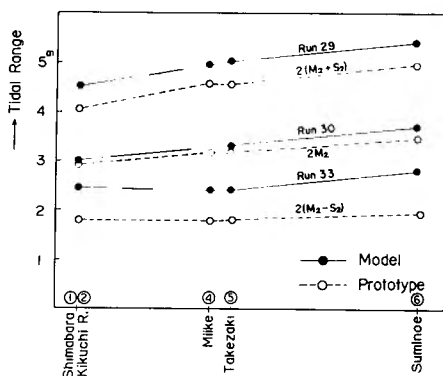


Fig. 9. Tidal range.

first and second term and the phase lag are tabulated.

The tidal range at each point is illustrated in Fig. 9. In this figure the black circle and full line show the value in the model, and the open circle and broken line the value in the prototype. The value of the spring tidal range $2(M_2 + S_2)$, the mean tidal range $2M_2$, and the neap tidal range $2(M_2 - S_2)$ are shown for the prototype.

(b) *Current ellipse*

The current ellipses at 4 points in the model were obtained by measuring the velocity by tracing a float.

Two examples at St. B and D are shown in Fig. 10 together with those of the prototype.

(c) *Flow pattern*

The flow pattern is illustrated in Fig. 11. In the flood the direction of the flow is the reverse and the velocity is almost the same.

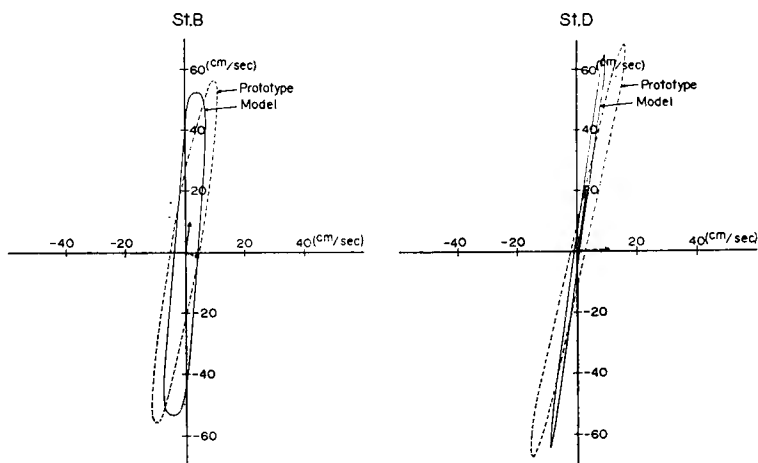


Fig. 10. Current ellipse.

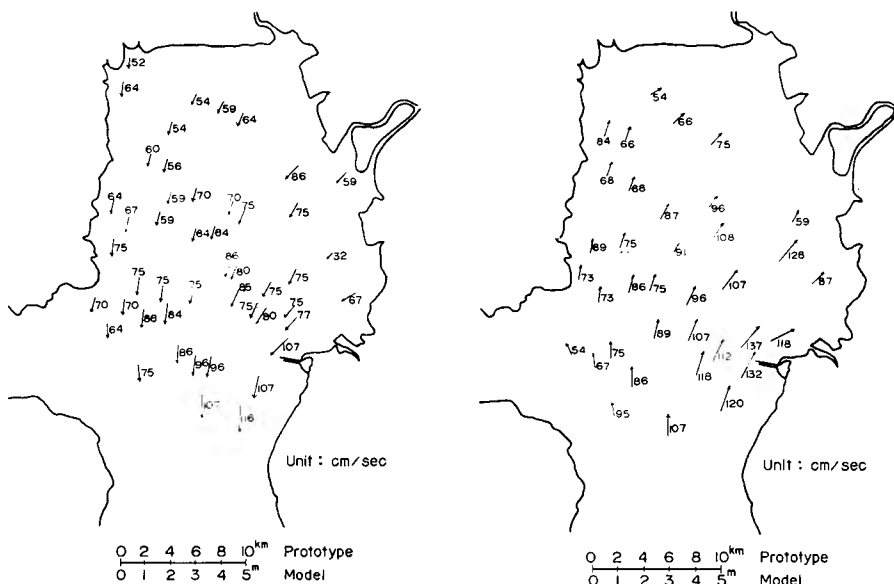


Fig. 11a. Flow pattern in the ebb.

Fig. 11b. Flow pattern in the flood.

(d) *Tidal locus*

An example of the orbits of the floats as they moved in one tidal cycle is shown in Fig. 12. The full line indicates the movement during the flood and the broken line the movement during the ebb. It is seen that the floats do not come back to their initial positions and some residues remain. When the directions of the vectors of these residues are the same, these may show the general flow. The residues are shown in the form of the mean velocity through one



Fig. 12. Tidal locus.

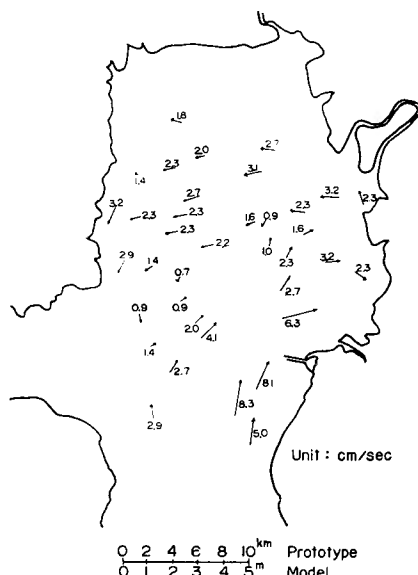


Fig. 13. Tidal residue.

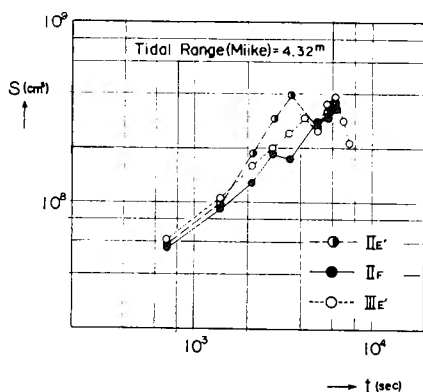


Fig. 14. Time change of the area of the dye patch.

cycle in Fig. 13.

(e) *Diffusion from an instantaneous point source*

The time change of the visual area of the dye patches, which were thrown at the mouth of Omura River and 1 km off it, was observed. The results are shown in Fig. 14. II and III are for the ebb, and IV and I are for the flood. The abscissa shows the duration time after putting the dye into the sea and the ordinate shows the area of the dye patch.

7. Consideration

(a) *Tide*

The water level in the model generally changes sinusoidally with exceptions of some secondary undulations at St. 4 and 6. It is considered that the reason for this is that these two stations are both situated in the innermost part of the shallow long channel and some resonance may occur.

In the inner part of the bay the tidal range increases about 20% as shown in the form of the ratio to St. 1 in Table 3. Since the second harmonic constant is in the order of several percent of the first one, although it increases in the inner part of the bay, under the distorting influence of the wave form, generally we may regard the tidal wave as sinusoidal. The state of increase of the tidal range is also illustrated in Fig. 9 both for the model and the prototype. From this figure it is clear that the tendency of the increase of the tidal range is well reproduced in the model. Therefore it can be considered as holding similitude with the tide.

(b) *Current ellipse*

From Fig. 10 it is clear that the current ellipses at St. B and D in the model show good agreement with the prototype although there are slight differences in the direction of the axis.

The general flow in the model does not coincide with that of the prototype. It may be illogical to compare them directly because there are some effects of the wind, the freshwater from the river and so on in the prototype, and they are not taken into account in the model.

(c) *Flow pattern*

From the comparison between Fig. 11 and Fig. 2 or 4, it is found that the flow pattern in the model accurately reproduces that in the prototype.

(d) *Tidal locus*

The tidal excursions in this area are in the order of 9~14 km as shown in Fig. 12, and are shorter in the inner part. It is considered that taking into account the effect of the tidal range the tidal excursions in the model agree well with the value 11 km in the prototype, which was obtained from the observation of the locus of the float.

The tidal residue shown in Fig. 13 represents one kind of general flow. This shows the general flow from the Lagrangean point of view, while that shown in Fig. 3 is from the Eulerian view. Although this is usually called the general flow, it also represents the general flow when the flow is uniform in the neighborhood. It is found that there is a large counterclockwise circulation in the inner part and a small clockwise one in the Omuta Area. In comparing

this with the one in the prototype shown in Fig. 3, it is found that the general tendency is almost exactly similar. However it is impossible to compare them quantitatively and in detail because there are no quantitative data in the prototype.

(e) *Diffusion from an instantaneous point source*

There are some examples in Fig. 14 which reproduce the area of the patch and the duration time before decreasing the area in the prototype shown in Fig.

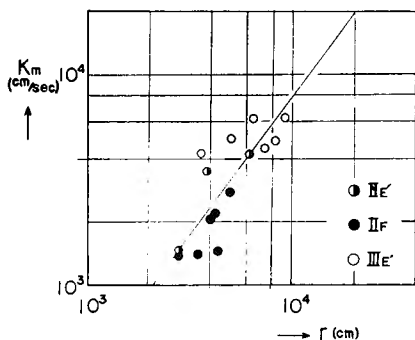


Fig. 15. Relation between the diffusion coefficient K_m and the equivalent radius r .

5. However, the rate of increase in the model is smaller than that in the prototype, and it suggests a weaker diffusion in the model.

Fig. 15 shows the diffusion coefficient in the model obtained through the same process as in the case of the prototype. The slope of the straight line is also $4/3$. Although the range of the data is small it seems to be better to draw a steeper line. In comparing this with Fig. 6, it is found that the diffusion coefficient in

the model is about $1/3$ of the prototype. This may be caused by the difference between the flow in the prototype and that in the model; that is, in the prototype the maximum Reynolds number is in the order of 10^7 and the turbulence grows violently while in the model the turbulence does not grow sufficiently. Further study is necessary to clarify this point.

8. Conclusion

By the present hydraulic model experiment, where the model used to represent the semidiurnal tide had a horizontal scale of $1/2000$ and a vertical scale of $1/200$ and where the effects of density stratification, waves and wind were disregarded, it is established that:

- (1) The tide involving the state of increase of the range in the innerpart of the bay is well reproduced.
- (2) The tidal current, that is, the current ellipses at 4 km off Omuta, and the flow pattern and the tidal excursion in the Omuta area, are well reproduced.
- (3) The general flow is considered to be generally reproduced.
- (4) The diffusion coefficient in the model is about $1/3$ of that in the prototype. This may be caused by the difference of the state of the flow in the prototype and the model. Further study is expected on this point.

It is considered that larger turbulence such as that of the scale of the tidal excursion may play a more important role in water pollution than smaller turbulence such as that of the scale of the dye patch. It is necessary to clarify this point through further experiment.

Acknowledgements

The author wishes to thank Professor Y. Iwagaki, Disaster Prevention Research Institute, Kyoto University, and Professor H. Kunishi, Geophysical Institute, Kyoto University, for their kind advice. Many thanks are also due to Mr. Y. Kitagawa for his assistance in the experiment.

This study was partly sponsored by the Ministry of International Trade and Industry.

References

- Arons, A. B. and H. Stommel, 1951 ; A mixing-length theory of tidal flushing, *Trans. Amer. Geoph. Union.*, 32, 419-421.
- Higuchi, H., 1963 ; On the hydraulic model experiment on nearshore tidal current. *Bulletin on Coastal Oceanography*, 2 (2), 14-17 (in Japanese).
- Hirano, T. and K. Sugiura, 1958 ; On the salinity distribution in a small bay with inflow from a river, *Bulletin of Tokai District Fisheries Research Institute*, 22, 1-15 (in Japanese).
- Hydrographic Division, 1955 ; Tidal current chart near Miike Harbor (in Japanese).
- Iwagaki, Y., 1953 ; Theory on open channel flow, *Recent Developments in Hydrotechnics*, 16 (in Japanese).
- Japan Meteorological Agency, 1965 ; Tide table 1966, 438 (in Japanese).
- Nagasaki Marine Observatory, 1959 ; Report on the Ariake Bay model experiment—On the tide in Ariake Bay, 1-67 (in Japanese).
- Nagasaki Marine Observatory, 1965 ; Marine observation accompanied with the investigation of water pollution (in Japanese).
- Nakano, M., 1940 ; The tide, *Kokon Shoin*, 481 p. (in Japanese).
- Takada, Y. and Y. Tohara, 1963 ; On the hydraulic model experiment of Ariake Bay (1), *Proc. 10th Conference of Coastal Engrs. in Japan*, 70-74 (in Japanese).
- Takada, Y. and Y. Tohara, 1963 ; Ditto (2), ditto 70-74 (in Japanese).